Pergamon

Biochemical Pharmacology, Vol. 49, No. 12, pp. 1759–1767, 1995.

0006-2952/95 $9.50 + 0.00

0006-2952(95)00087-9

PURIFICATION OF RECOMBINANT HUMAN *N*-ACETYLTRANSFERASE TYPE 1 (NAT1) EXPRESSED IN *E. COLI* AND CHARACTERIZATION OF ITS POTENTIAL ROLE IN FOLATE METABOLISM

A. WARD, M. J. SUMMERS and E. SIM*

Department of Pharmacology, University of Oxford, Mansfield Road, Oxford OX1 3QT, U.K.

(*Received* 13 *December* 1994; *accepted* 9 *February* 1995)

Abstract—Human arylamine *N*-acetyltransferase type 1 (NAT1) has been cloned from human genomic DNA, into the vector pET(5a) and expressed in *Escherichia coli*. The recombinant protein has been purified to apparent homogeneity using anion exchange chromatography. The arylamine acceptor specificity, and the effect of potential NAT1 inhibitors has been investigated using purified recombinant protein. The K_m of the recombinant NAT1 protein for the substrates *para*-aminobenzoate (*p*-aba) and 4-aminosalicylate are 14.3 and 11.8 μM, respectively. Folate and amethopterin were found to be potent competitive inhibitors of *p*-aba acetylation, with K_i values of 13.3 and 9.5 μM, respectively. The pteroate moiety of folate, in contrast is a poor inhibitor, with 100 μM pteroate inhibiting only 40% of NAT1 activity. A catabolite of folate *para*-aminobenzoly-L-glutamate has also been shown to be a NAT1 substrate with a K_m value of 263 μM.

Key words: human *N*-acetyltransferase type 1; amethopterin; folate; *para*-aminobenzoly-L-glutamate.

NAT† catalyses the N-acetylation of arylamines from acetyl-CoA [1]. The reaction is a classical two-step substituted enzyme (ping-pong) kinetic mechanism, in which the acetyl group is transferred first from the acetyl donor, acetyl-CoA, to the NAT enzyme and subsequently to the acceptor amine substrate [2].

Arylamines can also be N-hydroxylated by hepatic cytochrome P4501A2, and carcinogenic arylamines are converted to *N*-hydroxy-arylamine proximate carcinogens [3]. Following N-hydroxylation NAT can O-acetylate the *N*-hydroxy moiety, which results in the formation of highly unstable *N*-acetoxyarylamine metabolites. On hydrolysis the resulting arylnitrenium ions can form complexes with DNA. Such DNA adduct formation has been implicated in the production of malignant phenotypes [4].

NAT thus appears to have two opposing metabolic roles. N-Acetylation results in deactivating compounds for excretion [5], but in conjunction with cytochrome P450 N-hydroxylation of arylamines NAT can catalyse O-acetylation to produce activated carcinogens.

There are two isozymes of human NAT, NAT1 and NAT2, which are encoded at two loci on chromosome 8 [6]. The two isozymes share 87% sequence identity at the nucleotide level [7] and have overlapping but distinct substrate specificities. According to recently approved nomenclature [8] the most common human NAT1 allele is designated NAT1*3, and in this paper it is the NAT1*3 allele to which NAT1 refers.

NAT2 is expressed in the liver [9] and colonic epithelium [10], and is extensively involved in the metabolism of drugs including isoniazid, sulphamethazine and procainamide [11]. The NAT2 gene locus is polymorphic with at least six different alleles differing by a combination of up to three point mutations within the coding region [12]. One allele confers fast acetylation (NAT2*4), whilst all the others are associated with slow acetylation. The acetylator status of individuals has for many years been linked with predisposition to disease. Slow acetylators are at increased risk of arylamine induced bladder cancer [13, 14], and hydralazine induced immunotoxicity [15].

NAT1 has a widespread tissue distribution, being found in the liver [16], bladder [17], erythrocytes [18], brain [19] and lymphocytes [20]. Substrates of NAT1 include *p*-aba, 4-ASA, and sulphamethoxazole [21, 22] and in common with NAT2, the carcinogens 2-aminofluorene and benzidine. To date no endogenous substrate for either isozyme has been identified.

There is one major NAT1 allele but others have also been described at this locus [23]. Functional variation in NAT1 activity has also been described [24, 25]. It is not clear what the relationship is between the allelic variants of NAT1 and inter-individual variation in NAT1 activity. It has

* Corresponding author. Tel. (01865) 271596; FAX (01865) 271853.

† Abbreviations: NAT, arylamine *N*-acetyltransferase; NAT1, human arylamine *N*-acetyltransferase type 1 (NAT1*3); HPLC, high-pressure liquid chromatography; *p*-aba, *para*-aminobenzoate; 4-ASA, 4-aminosalicylate; DTT, dithiothreitol; PCR, polymerase chain reaction; IPTG, isopropyl-β-D-thiogalactopyranoside; NAT2, human arylamine *N*-acetyltransferase type 2 (NAT2*4).

previously been suggested that endogenous inhibitors, possibly folate, could contribute to the observed functional variation in NAT1 activity. NAT1 constitutes at maximum only 0.005% of total cell protein [16] and so human NAT1 has been purified after cloning and expression in *E. coli*. The recombinant protein has been used to investigate further the characteristics of substrates and potential inhibitors of NAT1.

MATERIALS AND METHODS

Restriction endonucleases and other DNA-modifying enzymes were purchased from Boehringer Mannheim (Lewes, Sussex, U.K.) with the exception of Native Pfu polymerase which was obtained from Stratagene (Cambridge, U.K.). Oligonucleotide primers were synthesized by Mrs V. Cooper (Dyson Perrins Laboratory, University of Oxford, U.K.). The Novagen expression vector pET(5a) and *E. coli* glycerol stocks were purchased from NBL Gene Sciences Ltd (Cramlington, U.K.). A gene clean II kit was purchased from Stratech Scientific (Luton, U.K.). All chemicals and buffers were purchased from either Sigma (Poole, U.K.) or Aldrich (Gillingham, U.K.), except where stated. HPLC grade acetonitrile and acetic acid were purchased from Rathburn Chemicals (Walkerburn, U.K.). *N*-Acetamidosalicylic acid and *N*-acetamidobenzoyl-L-glutamic acid were synthesized as previously described [26]. All chromatographic media were purchased from Pharmacia (St. Albans, U.K.), with the exception of the DEAE MemSep anion exchange cartridge which was from Millipore (Watford, U.K.). A dye binding kit, for the estimation of protein content, was purchased from Biorad (Hemel Hempstead, U.K.).

Plasmid construction. The coding region of human NAT1 was amplified by the PCR using 2.5 U Native Pfu polymerase, 1 μg genomic DNA as template and 50 pmol each of a pair of oligonucleotide primers, NatHu22 ACTCC*GAATTC*TAAATAG-TAAAAA (antisense) and NatHu23 TAAGGGG-*CATATG*GACATTGAA (sense), which introduce the restriction enzyme sites NdeI and EcoRI (underlined). The mismatches created which generate the restriction enzyme sites are shown in italics. Thirty-five cycles of amplification were carried out as follows: denaturation: 95°, 5 min; annealing: 54°, 5 min; and extension: 75°, 2 min.

The DNA product was separated by electrophoresis on a 1% (w/v) agarose gel, and isolated using a silica matrix (Geneclean II kit).

The NAT1 coding region was then inserted into the pET(5a) expression plasmid vector at the NdeI and EcoRI sites. The plasmid was initially established in the *E. coli* strain NM554, which lacks a chromosomal copy of the T7 RNA polymerase gene.

The cloned NAT1 was sequenced using methods and primers [23] as previously described [27].

Expression. Plasmid produced in the *E. coli* strain NM554 was used to transform either the *E. coli* strain BL21(DE3)pLysS or BL21(DE3), for the production of recombinant protein. Both strains of *E. coli* have inserted into their *int* gene a fragment of DNA containing the *lacI* gene, the *lacUV5* promoter and the gene for T7 RNA polymerase. The *lacUV5* promoter is inducible by isopropyl-β-D-thiogalactopyranoside (IPTG). Addition of IPTG to a growing culture induces the T7 RNA polymerase, which in turn transcribes the target DNA in the plasmid.

Escherichia coli were grown at 37° in L-broth with 50 μg/mL ampicillin, and were induced at mid-log phase with 0.4 mM IPTG for 4 hr. Cultures with volumes greater than 1L were grown by S. Cole (Oxford Centre for Molecular Science, University of Oxford, U.K.) using the same conditions, except that cells were induced with 0.1 mM IPTG. Following induction cells were harvested by centrifugation (3000 rpm, 4°, 20 min). The cell pellet was then resuspended in 20 mM Tris/HCl, 1 mM EDTA, 5 mM DTT and 1 mM pefabloc (S. Black (U.K.) Import/Export). Except where indicated cell lysis was induced by freezing once in liquid nitrogen and then thawing at 37°, for the *E. coli* strain BL21(DE3)pLysS, or by sonication (10 sec) for the *E. coli* strain BL21(DE3). The recombinant soluble protein was recovered after DNAse treatment, and centrifugation (10,000 rpm, 4°, 30 min Sorval SS34 rotor) to remove cell debris.

The recovered soluble protein was retained for determination of NAT1 activity. In order to determine whether there were any aggregated insoluble NAT1 (inclusion bodies) associated with the cell debris, the cell debris from 250 mL of bacterial culture was resuspended in 10 mL of 0.5% Triton X100, 1 mM EDTA, and centrifuged (5000 rpm, 4°, 10 min). The insoluble material was washed twice more with 0.5% Triton X100, 1 mM EDTA, and was finally resuspended in 1 mL phosphate buffered saline.

Chromatographic purification of recombinant NAT1. Bacterial cell lysate (0.2–0.5 g protein, corresponding to approximately 500 mL bacterial culture) was loaded at 4° onto a column of Q-Sepharose 'fast flow' (1.6 × 32 cm), and run at a flow rate of 2.5 mL/min on a Pharmacia FPLC system. The column was washed with 20 mM Tris/HCl, 1 mM EDTA, 5 mM DTT, 0.5 mM pefabloc pH 7.5. A linear gradient of 500 mL 0–500 mM NaCl was then applied in the same buffer. Fractions of 10 mL were collected, and 50 μL of each was assayed for NAT1 activity using 1 mM *p*-aba as substrate. Fractions containing NAT1 were desalted using a 50 mL Sephadex G25 column.

The desalted NAT1 fractions were then applied to a DEAE MemSep anion exchange cartridge, and the cartridge was washed (5 mL/min) with 20 mM Tris/HCl pH 7.5, 1 mM EDTA, 5 mM DTT, 0.5 mM pefabloc. A linear gradient of 200 mL 0–75 mM NaCl was developed in the same buffer. Fractions of 5 mL were collected.

For larger scale purifications corresponding to 1–2L of bacterial culture a further purification step on a Superdex 75 gel filtration column (2.6 × 46 cm) was carried out after Q-Sepharose. The Superdex 75 column was washed with 300 mL of 20 mM Tris/HCl pH 7.5, 1 mM EDTA, 5 mM DTT and 0.5 mM pefabloc at a flow rate of 2 mL/min. Fractions of 4 mL were collected, and aliquots were assayed for NAT1 activity with 1 mM *p*-aba as substrate.

Enzymatic assays. *N*-Acetyltransferase activity in supernatants after bacterial cell lysis was determined using a spectrophotometric assay as described previously [24] with 1 mM *p*-aba as substrate.

The method was modified for HPLC analysis as follows. In a total volume of 90 μL; 50 μL of purified recombinant NAT1 (up to 4 ng protein) in 20 mM Tris/HCl, 1 mM EDTA, 5 mM DTT containing 0–180 μM folate or amethopterin was mixed with 20 μL of an acetyl-CoA/phosphotransacetylase regenerating system (200 mM Tris/HCl, 4 mM EDTA, 22 mM acetyl phosphate, 4 mM DTT, 2.2 U/mL phosphotransacetylase and 450 μM acetyl-CoA), and pre-incubated at 37° for 3 min. Substrate was then added in 20 μL water, to start the reaction. The conversion of substrate was measured over 5 min at 37°, and was terminated by the addition of 10 μL 15% (v/v) perchloric acid. Precipitated protein was pelleted by centrifugation (3 min, 13,500 rpm, 4°) and tubes were placed on ice for less than one hour prior to analysis. Assays with *para*-aminobenzoyl-L-glutamate as substrate used 0.15 μg purified recombinant NAT1 protein. In all assays the condition of linearity was met.

Formation of N-acetylated products was quantified by HPLC (Waters 600E System Controller and 484 Tunable Absorbance Detector; Millipore Corporation, Milford, U.S.A.) using a semi-preparative reverse-phase C18 column. Ten or 20 μL of each assay supernatant was injected. HPLC conditions were as follows: UV detection at 266 nm and a flow rate of 2 mL/min, except that 1 mL/min was used for *para*-aminobenzoyl-L-glutamate. The mobile phases used were 50 mM acetic acid, acetonitrile (90:10) for *p*-aba (2.8 min), *N*-acetyl*p*-aba (5 min), folate (4.4 min), 4-ASA (3.4 min), *N*-acetyl 4ASA (5.2 min), *para*-aminobenzoyl-L-glutamate (4.2 min) and *N*-acetyl-*p*-aminobenzoyl-L-glutamate (7.2 min). The retention times are shown in brackets after each compound. For *p*-aba and *N*-acetyl-*p*-aba, in the presence of amethopterin and pteroate the mobile phase was 50 mM acetic acid/acetonitrile (92:8), giving retention times of 3.2 min for *p*-aba, 6.5 min for *N*-acetyl-*p*-aba, 8.8 min for amethopterin and 10.4 min for pteroate. Kinetic parameters (K_m, K_i and V_{max}) were determined from Lineweaver–Burk plots. Protein concentrations were measured using a Bradford dye binding assay with human γ-globulin as a standard [28].

Electrophoretic analysis of recombinant NAT1. Both the bacterial cell lysate and purified fractions were analysed by electrophoresis on 10% (w/v)

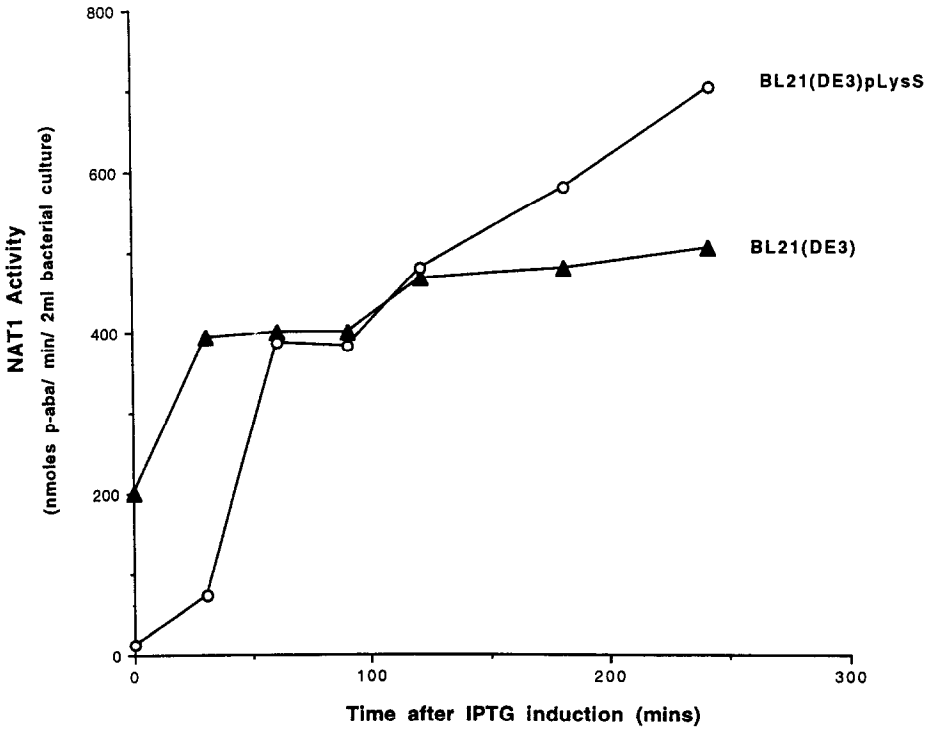

Fig. 1. Comparison of NAT1 expression in the *E. coli* strains BL21(DE3) and BL21(DE3)pLysS. Cultures (250 ml) of BL21(DE3) and BL21(DE3)pLysS, carrying the NAT1/pET(5a) vector construct (Fig. 1), were grown in L-broth containing 50 μg/ml ampicillin, at 37° with shaking. Once the absorbance at 600 nm had reached 0.6 (mid-log phase) cells were induced by the addition of IPTG to a final concentration of 0.4 mM. At the times indicated after induction 2 mL aliquots of culture were withdrawn. Cells were collected by centrifugation (3000 rpm, 4°, 10 min) and resuspended in 200 μL 20 mM Tris-HCl, 5 mM DTT, 1 mM EDTA, 0.5 mM pefabloc (pH 7.5). Cells were then lysed, as described and the cell debris removed by centrifugation. Supernatants were assayed for NAT1 activity as described. NAT1 activity recovered from the *E. coli* strain BL21(DE3) is depicted by the closed triangles, and from the strain BL21(DE3)pLysS by the open circles.

polyacrylamide Tris/tricine gel containing 0.1% (w/v) SDS [29]. Gels were either stained with silver [30] or Coomassie blue.

RESULTS

Expression

Human NAT1 was expressed successfully in the *E. coli* strains BL21(DE3) and BL21(DE3)pLysS. As Fig. 1 shows more NAT1 is being expressed, and can be recovered, from the pLysS strain which has proved to be of great use in developing a purification strategy.

The *E. coli* strain BL21(DE3)pLysS expresses T7 lysozyme [31]. Relatively high levels of T7 lysozyme can be tolerated by the bacteria as the protein is unable to pass through the inner membrane to reach the peptidoglycan layer. Treatments which disrupt the inner membrane, but would not normally result in lysis, such as freeze–thaw and osmotic shock, induce rapid lysis in cells containing T7 lysozyme. It has been possible, therefore, to lyse cells recovered from 500 mL of bacterial culture in 5 mL of buffer using one cycle of freezing and thawing. This produces a concentrated source of protein without the need for ammonium sulphate precipitation which results in high losses of NAT1 activity [32].

All NAT1 activity, expressed in either strain of bacteria, was found to be soluble. This was confirmed by the absence on SDS-PAGE of any insoluble material corresponding to NAT1, which migrates with an apparent molecular weight of 33 kDa.

Purification

Recombinant NAT1 was successfully isolated (Table 1), after 100-fold purification, using two anion exchange chromatographic steps. Figure 2 shows the results of the first purification step on Q-Sepharose. NAT1 elutes as a single protein peak at around 100 mM NaCl. The recovery of the total activity is 75% in this step, and 42% is in the peak fraction. When the material from the Q-Sepharose step is applied to a MemSep anion exchange cartridge NAT1 elutes at 20 mM NaCl. Analysis of the eluted fractions by SDS-PAGE gel electrophoresis shows that the NAT1 has been purified to apparent homogeneity (Fig. 3).

Purification of NAT1 on a larger scale after anion exchange on Q-Sepharose and gel filtration on Superdex 75, results in NAT1 which has been purified 57-fold (Table 1).

Enzymology

The kinetic properties of NAT1 were characterized using partially purified recombinant NAT1 (Table 1). The apparent K_m values are 14.3 μM for *p*-aba and 11.8 μM for 4-ASA. These values are in broad agreement with K_m values measured for NAT1 derived from human tissue sources. NAT1 partially purified from human liver has K_m values of 12 μM

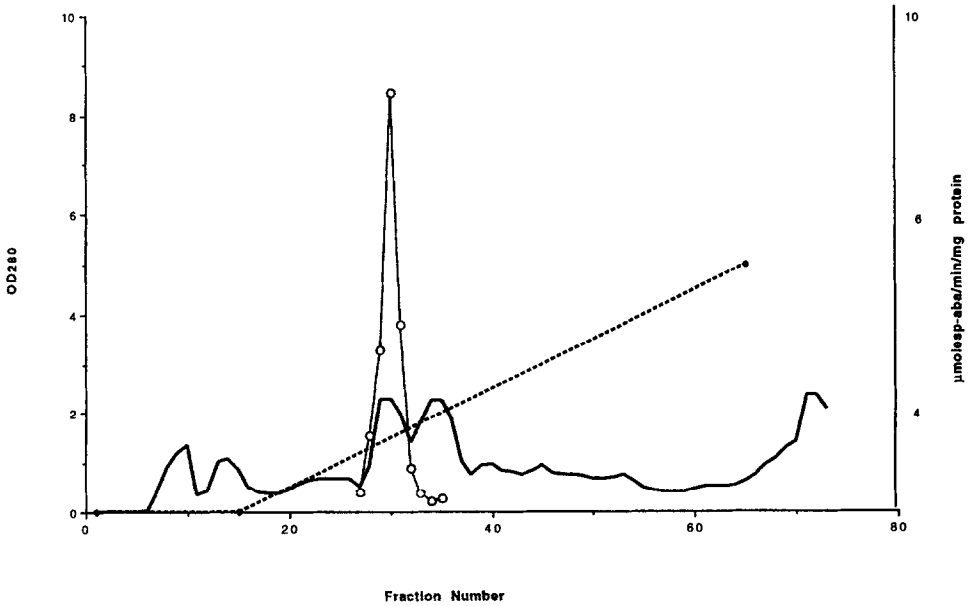

Fig. 2. Purification of NAT1 on Q-Sepharose. Cells from 400 mL of BL21(DE3)pLysS culture were resuspended in 62 mL of buffer A (20 mM Tris/HCl, 1 mM EDTA, 5 mM DTT and 0.5 mM pefabloc (pH 7.5)), which lyses the cells by osmotic shock. The recovered soluble protein was then applied to a column of Q-Sepharose (32 × 1.6 cm). The column was washed with 70 mL of Buffer A prior to the application of a 500 mL 0–500 mM NaCl gradient, in the same buffer. Fractions of 10 mL were collected. The absorbance at 280 nm is indicated by the solid line. Fractions were assayed for NAT1 activity (open circles) using 1 mM *p*-aba and 0.44 mM acetyl-CoA as substrates. The NaCl gradient is indicated by the dotted line. The desalted peak Q-Sepharose fraction was then applied to a DEAE MemSep anion exchange cartridge.

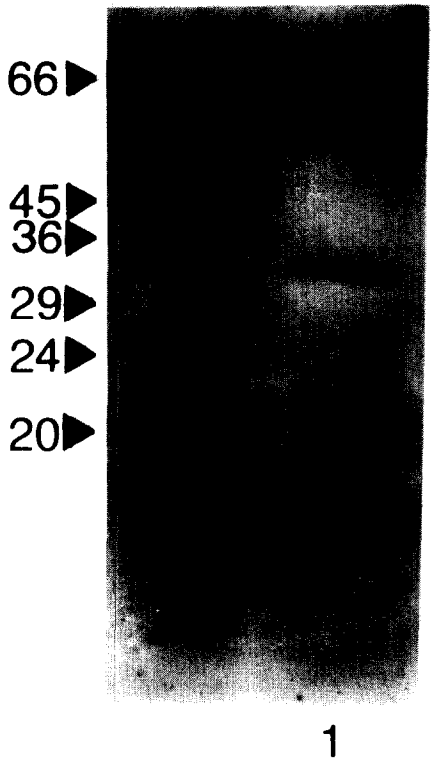

Fig. 3. Silver stained 10% (w/v) polyacrylamide Tris-tricine gel, showing purified recombinant NAT1. The desalted peak fraction from the Q-Sepharose purification shown in Fig. 2 was applied to a Mem Sep HP1010 anion exchange cartridge, and washed with 25 mL of 20 mM Tris-HCl, 1 mM EDTA, 5 mM DTT and 0.5 mM pefabloc (pH 7.5). A linear gradient of 0–75 mM NaCl was then developed in 200 mL of the same buffer. Track 1 corresponds to the fraction eluted at 20 mM NaCl. The closed arrow heads indicate the molecular weight markers in kDa.

for *p*-aba and 9 μM for 4-ASA [32]. Crude soluble fractions of human leukocytes, which only express NAT1, have K_m values in the range of 12–14 μM for *p*-aba [25]. *para*-Aminobenzoyl-L-glutamate was also demonstrated to be a NAT1 substrate with a K_m value of 263 μM.

We have also characterized the inhibition of partially purified NAT1 and shown that both folate and amethopterin are competitive inhibitors with respect to *p*-aba N-acetylation. The K_i values were calculated (Fig. 4a and b) to be 13.3 μM for folate, and 9.5 μM for amethopterin. Pteroate is a much poorer inhibitor than either folate or amethopterin. When the compounds are compared as inhibitors of *p*-aba N-acetylation, pteroate gives only approximately 50% of the inhibition observed with folate and amethopterin (Fig. 4c).

DISCUSSION

In the present study it has been demonstrated that the recombinant human NAT1 catalyses the N-acetylation of substrates with Michaelis constants that are in good agreement with those determined previously with NAT1 purified from human tissue sources [25, 32], showing that the expressed protein

Table 1. Purification of recombinant NAT1 from BL21(DE3)pLysS bacterial culture

Fraction	Total protein (mg)	Total activity (nmoles *p*-aba/min)	Protein recovery (%)	Yield activity (%)	Specific activity (nmoles *p*-aba/min/mg protein)	Fold purification
(a) 500 mL of BL21(DE3)pLysS						
Lysate	200	461,638	100	100	2308	1
Q-Sepharose (peak fraction)	22.8	192,771	11.4	42	8454	3.7
Mem Sep	0.13	33,000	0.065	7.2	253,846	110
(b) 1.6 L of BL21(DE5)pLysS						
Lysate	1000	904,800	100	100	904	1
Q-Sepharose (pool)	53.4	532,800	5.34	59	9984	11
Superdex 75	1.2	61,360	0.12	6.8	51,133	57

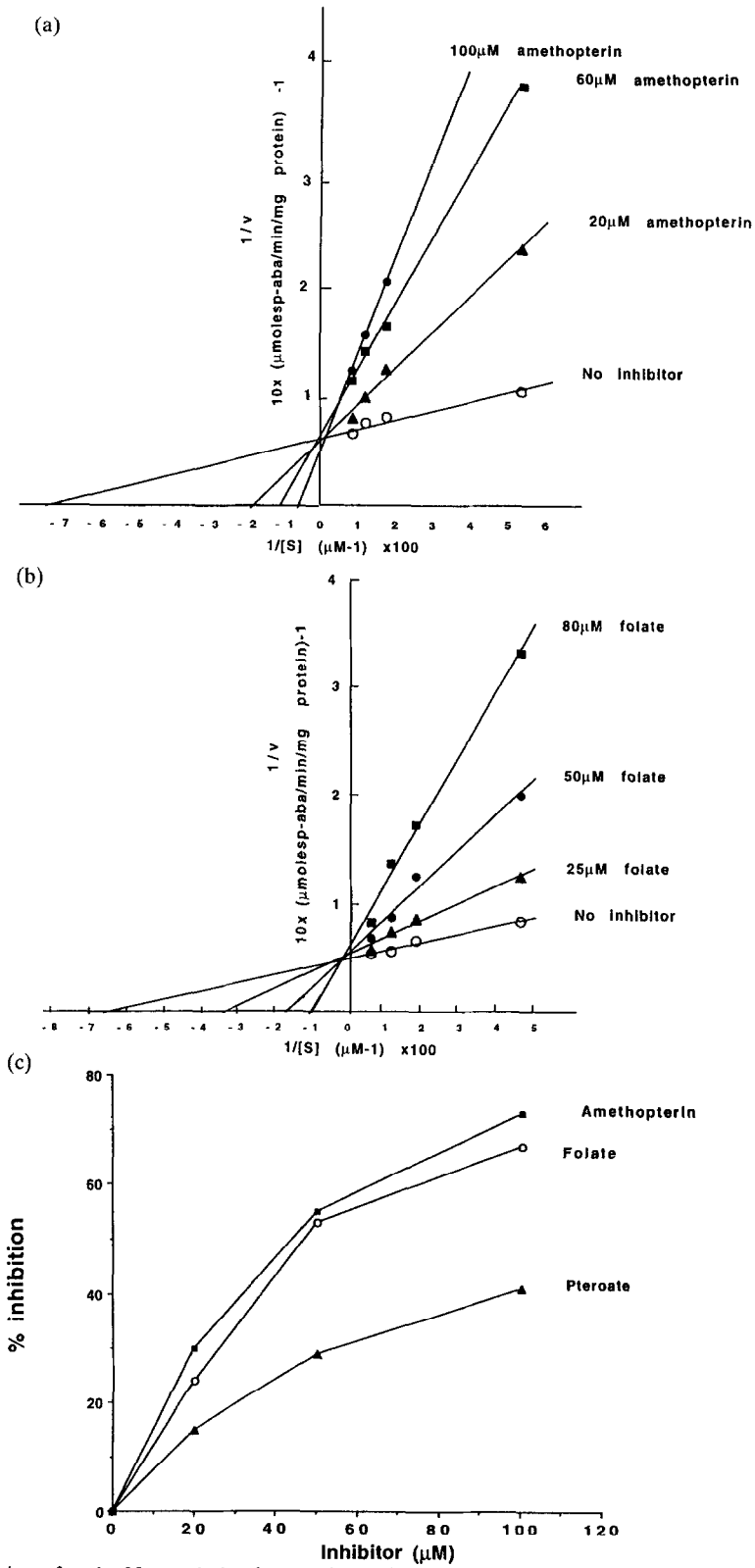

Fig. 4. Inhibition of *p*-aba N-acetylation by amethopterin and folate. NAT1 activity using 3 ng protein from the peak fraction of Superdex 75 was assayed over 5 min as described in the Methods section. The reaction was started with 90, 225, 450 or 675 μM *p*-aba as substrate. The substrates and products were separated on HPLC. The mobile phases were as outlined in Table 1. Lineweaver–Burk plots are shown for (a) amethopterin, and (b) folate. (c) Inhibition of NAT1 by folate, amethopterin and pteroate. All reactions were started by the addition of *p*-aba to a final concentration of 150 μM. The uninhibited activity in (c) was measured to be 17.8 μmols *p*-aba acetylated/min/mg protein.

is a good model for NAT1 *in vivo*. The folate catabolite *p*-aminobenzoyl-L-glutamate has also been demonstrated to be a substrate for NAT1, with a K_m value of 263 μM.

Previous kinetic studies with the folate antagonist, and chemotherapeutic agent, amethopterin have been performed by Jacobson [33] and Andres [34], using pigeon liver as the source of NAT. Both reported non-competitive inhibition with the acceptor amine *p*-nitroaniline. Jacobson also found large discrepancies between the inhibitory potencies of amethopterin and folate, with folate being a much weaker inhibitor. Erythrocyte NAT1 activity, with *p*-aba as a substrate, has been shown to be competitively inhibited by amethopterin [35] and folate [36]. The K_i values were 10 μM for folate and 60 μM for amethopterin. However, there are difficulties in interpreting this data as NAT1 accounts for 0.005% of total protein present in the cell, and folate is known to bind electrostatically to many proteins, including haemoglobin. By using purified recombinant NAT1 the electrostatic binding of folate to other proteins can effectively be discounted, and therefore the true nature of the inhibition can be determined.

Folate, and the related compound amethopterin, are shown here to be competitive inhibitors of NAT1; both inhibit with similar potencies when measured as inhibitors of *p*-aba N-acetylation.

Amethopterin is a folate antagonist and is administered as a chemotherapeutic agent for the treatment of leukaemias [37]. Amethopterin blocks the synthesis of deoxythymidylate by competitively inhibiting dihydrofolate reductase in the nanomolar range. The inhibition of dihydrofolate reductase prevents the conversion of dihydrofolate to tetrahydrofolate, this in turn prevents the synthesis of N^5, N^{10}-methylenetetrahydrofolate which acts as a methyl donor to convert deoxyuridylate to deoxythymidylate [38].

In vitro experiments have been carried out to investigate the uptake of amethopterin by erythrocytes [39] resuspended in plasma containing 0.1 mM amethopterin, which reflects the concentration of the drug achieved during high dose chemotherapy. Amethopterin in the erythrocytes only accumulated to a concentration of 0.5 μM. Therefore, the concentration of amethopterin likely to be reached *in vivo* is 0.5 μM. This concentration is below the K_i for inhibition of NAT1 by amethopterin, measured here as 9.5 μM. Therefore it is likely that NAT1 will be inhibited by less than 0.5% by amethopterin during chemotherapy, and so inhibition of NAT1 is unlikely to contribute to the chemotherapeutic role of amethopterin.

The central portion of both folate and amethopterin is *p*-aba (Fig. 5). It therefore seemed possible that inhibition of NAT1 by folate and amethopterin could be mediated through this portion of the molecule. However, pteroate (*p*-aba conjugated with a pteridine ring) (Figs 4c and 5) is a much less potent inhibitor of NAT1. This would indicate that folate and amethopterin do not interact with NAT1 through the *p*-aba portion of their structure, and that it is the negatively charged glutamate tail, which is missing in pteroate, which is important for interaction

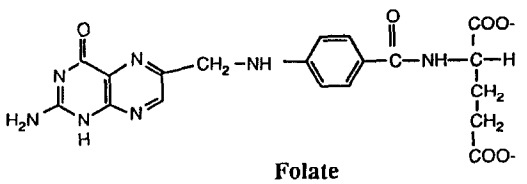

Folate

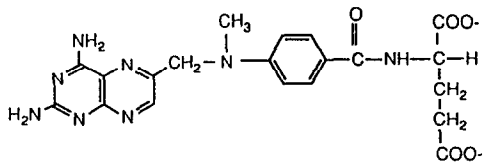

Amethopterin

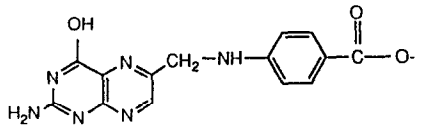

Pteroate

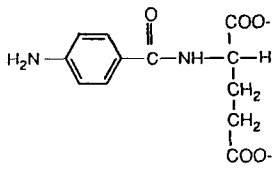

para-aminobenzoyl-L-glutamate

Fig. 5. The chemical structures of folate, amethopterin, pteroate and *p*-aminobenzoyl-L-glutamate. The folate structure is illustrated in the keto form.

with the active site of NAT1. This is supported by the finding that *para*-aminobenzoyl-L-glutamate is a NAT1 substrate. *In vivo* folate exists inside cells in multiple polyglutamated forms [40, 41]. In view of the likely interaction of the glutamate moiety with NAT1 it will be important to investigate the effects of the different polyglutamated folates on NAT1 activity. The purified enzyme will allow this interaction to be investigated.

In vivo the concentration of all folates in erythrocytes has been estimated to be between 1 and 2 μM [24, 42], but these values may be inaccurate in view of the indirect methods used for estimating the concentration. The K_i measured here for inhibition of NAT1 by folate is 13.3 μM. However, the K_m of NAT1 for *p*-aminobenzoyl-L-glutamate, a catabolite of folate, is 263 μM. *p*-Aminobenzoyl-L-glutamate is acetylated *in vivo* since *p*-acetamidobenzoyl-L-glutamate is found in the urine of rats [43] and humans [44]. Therefore, the concentration of folate inside cells is likely to have an effect on the amount of *p*-aminobenzoyl-L-glutamate which can be acetylated. There is likely

to be a balance between the effect on NAT1 of the concentration of folate and its breakdown product *p*-aminobenzoyl-L-glutamate. This could explain the observation that in rats [45] the degree of acetylation of *p*-aminobenzoyl-L-glutamate, measured by the urinary excretion of *p*-acetamidobenzoyl-L-glutamate, increases over a period of eight days after administration of a single dose of tritiated folate.

Folate deficiency syndromes as seen during malignancy [46] or pregnancy [47] may also be related to NAT1 activity. During pregnancy there is an increased demand for folate, which cannot be accounted for by transfer of folate from the mother to the foetus. In pregnancy there is accelerated folate catabolism as the excreted concentration of *p*-acetamidobenzoyl-L-glutamate rises during the second trimester, but returns to normal postpartum [47]. It has been demonstrated that *p*-aminobenzoyl-L-glutamate is not a substrate for NAT2 [48], and therefore the data on *p*-acetamidobenzoyl-L-glutamate excretion in pregnancy suggest that NAT1 activity may increase. Hormonal changes which take place during pregnancy may play a part in the upregulation of NAT1, as it has been demonstrated that glucocorticoids induce hepatic NAT in rats [49]. Increased NAT1 activity in the mother may have a protective effect in preventing the transfer of potentially carcinogenic or toxic arylamines to the foetal circulation. The placenta, the major barrier between the maternal and foetal circulation also expresses NAT1 [50, 51], which may further protect the foetus.

NAT1, like folate, has a widespread tissue distribution. From studies presented here using purified recombinant human NAT1 enzyme it appears that the role of NAT1 may be to catalyse the acetylation of the folate breakdown product *p*-aminobenzoyl-L-glutamate, and that the amount of this breakdown product is a balance between NAT1 activity and the intracellular concentration of folate.

Acknowledgements—The authors thank the Wellcome Trust for financial support, Mrs A. Watson for technical assistance and S. Edmonds, Dr P. Thygesen, Dr L. Stanley, Angela Risch and John Sinclair for helpful discussion.

REFERENCES

1. Andres HH, Klem AJ, Szabo SM and Weber WW, New spectrophotometric & radiochemical assays for acetyl-CoA: Arylamine *N*-acetyltransferase applicable to a variety of arylamines. *Anal Biochem* **145**: 367–375, 1985.
2. Weber WW and Cohen SN, *N*-Acetylation of drugs: isolation and properties of *N*-acetyltransferase from rabbit liver. *Mol Pharmacol* **3**: 266–273, 1967.
3. Josephy DP, Towards the construction of the micromouse: bacterial strains expressing recombinant acetyltransferases. Abstract from *The 10th International Symposium on Microsomes & Drug Oxidations, Toronto, Canada*, 1994.
4. Vineis P, Bartsch H, Caporaso N, Harrington AM, Kadlubar FF, Landi MT, Malaveille C, Sheilds PG, Skipper P, Talaska G and Tannenbaum SR, Genetically based *N*-acetyltransferase metabolic polymorphism and low level environmental exposure to carcinogens. *Nature* **369**: 154–156, 1994.
5. Hein DW, Doll MA, Ruston TD, Gray K, Feng Y, Ferguson RJ and Grant DM, Metabolic activation and deactivation of arylamine carcinogens by recombinant human NAT1 and polymorphic NAT2 acetyltransferases. *Carcinogenesis* **14**: 1633–1638, 1993.
6. Hickman D, Risch A, Buckle V, Spurr NK, Jeremiah SJ, McCarthy A and Sim E, Chromosomal localization of human genes for arylamine *N*-acetyltransferase. *Biochem J* **297**: 441–445, 1994.
7. Blum M, Grant DM, McBride W, Heim M and Meyer UA, Human arylamine *N*-acetyltransferase genes—Isolation, chromosomal localization and functional expression. *DNA Cell Biol* **9**: 193–203, 1990.
8. Vatsis KP *et al.*, Nomenclature for the *N*-acetyltransferases. *Pharmacogenetics* **5**: 1–17, 1995.
9. Deguchi T, Sequences and expression of alleles of polymorphic arylamine *N*-acetyltransferase of human liver. *J Biol Chem* **267**: 18140–18147, 1992.
10. Ilett KF, Ingram DM, Carpenter DS, Teilett CH, Lang NP, Kadlubar FF and Minchin RF, Expression of monomorphic and polymorphic N-acetyltransferases in human colon. *Biochem Pharmacol* **47**: 914–917, 1994.
11. Ohsako S and Deguchi T, Cloning and expression of cDNA's for polymorphic and monomorphic arylamine *N*-acetyltransferases from human liver. *J Biol Chem* **265**: 4639–4634, 1990.
12. Hickman D, Risch A, Camilleri JP and Sim E, Genotyping human polymorphic arylamine *N*-acetyltransferase: identification of new slow allotypic variants. *Pharmacogenetics* **2**: 217–226, 1992.
13. Cartright RA, Glasham RW, Rogers HJ, Ahmed RA, Hall DB, Higgins E and Kahn MA, Role of *N*-acetyltransferase phenotypes in bladder carcinogenesis: A pharmacogenetic epidemiological approach to bladder cancer. *Lancet* **ii**: 842–846, 1982.
14. Risch A, Wallace DM, Bathers S and Sim E, Slow *N*-acetylation genotype is a susceptibility factor in occupational and smoking related bladder cancer. *Human Molec Genet* **4**: 231–236, 1995.
15. Perry HM, Ton EM, Carmody S and Sakamoto A, Relationship of acetyl transferase activity to antinuclear antibodies and toxic symptoms in hypertensive patients treated with hydralazine. *J Lab Clin Med* **76**: 114, 1970.
16. Grant DM, Lottspeich F and Meyer UA, Evidence for two closely related isozymes of arylamine *N*-acetyltransferase in human liver. *FEBS Lett* **244**: 203–207, 1989.
17. Coroneos E and Sim E, Arylamine *N*-acetyltransferase activity in human cultured cell lines. *Biochem Soc Trans* **19**: 129S, 1991.
18. Blondheim SH, Acetylation by blood cells. *Arch Biochem Biophys* **55**: 365–372, 1955.
19. Pacifici GM, Bencini C and Rane A, Acetyltransferase in humans: Development and tissue distribution. *Pharmacology* **32**: 283–291, 1986
20. Drayer DE, Strong JM, Jones B, Sandler A and Reidenberg MM, *In vitro* acetylation of drugs by human blood cells. *Drug Metab Dispos* **2**: 499–505, 1974.
21. Hutabarat RM, Smith AL and Unadkat JD, Disposition of drugs in cystic fibrosis. VII. Acetylation of sulphamethoxazole in blood cells. *In vitro–in vivo* correlation and characterization of its kinetics of acetylation in lymphocytes. *Clin Pharmacol Ther* **55**: 427–433, 1994.
22. Cribb AE, Nakamura H, Grant DM, Miller DM, Miller MA and Spielberg SP, Role of polymorphic and monomorphic human arylamine *N*-acetyltransferases in determining sulfamethoxazole metabolism. *Biochem Pharmacol* **45**: 1277–1282, 1993.
23. Vatsis KP and Weber WW, Structural heterogeneity of caucasian *N*-acetyltransferase at the NAT1 gene locus. *Arch Biochem Biophys* **301**: 71–76, 1993.

24. Ward A, Hickman D, Gordon JW and Sim E, Arylamine *N*-acetyltransferase in human red blood cells. *Biochem Pharmacol* **44**: 1099–1104, 1992.
25. Cribb AE, Grant DM, Miller MA and Spielberg SP, Expression of monomorphic arylamine *N*-acetyltransferase (NAT1) in human leukocytes. *J Pharmacol Exp Ther* **259**: 1241–1246, 1991.
26. du Souich P, Lalka D, Slaughter R, Elvin AT and McClean AJ, Mechanisms of non-linear disposition kinetics of sulphamethazine. *Clin Pharmacol Ther* **25**: 172–183, 1979.
27. Kelly SL and Sim E, Arylamine *N*-acetyltransferase in Balb/c mice: Identification of a novel mouse isoenzyme by cloning and expressing *in vitro*. *Biochem J* **302**: 347–353, 1994.
28. Bradford MM, A rapid and sensitive method for the quantitation of microgram quantities of protein utilizing the principle of protein–dye binding. *Anal Biochem* **72**: 248–254, 1976.
29. Schagger H and Von Gagow G, Tricine–sodium dodecyl sulphate polyacrylamide gel electrophoresis for the separation of proteins in the range 1–100 kDa. *Anal Biochem* **166**: 368–379, 1987.
30. Morrissey JH, Silver stain for proteins in polyacrylamide gels: A modified procedure with enhanced uniform sensitivity. *Anal Biochem* **117**: 307–310, 1981.
31. Studier FW, Use of bacteriophage T7 lysozyme to improve an inducible T7 expression system. *J Molec Biol* **219**: 37–44, 1991.
32. Grant DM, Blum H, Beer M and Meyer UA, Monomorphic and polymorphic human arylamine *N*-acetyltransferase: A comparison of liver isozymes and expressed products of two cloned genes. *Molec Pharmacol* **39**: 184–191, 1990.
33. Jacobson KB, Inhibition of acetyl transfer by amethopterin. *J Biol Chem* **235**: 2713–2716, 1960.
34. Andres HH, Kolb HJ and Weiss L, Purification and physical–chemical properties of acetyl-CoA: Arylamine *N*-acetyltransferase from pigeon liver *Biochem Biophys Acta* **746**: 182–192, 1983.
35. Motulsky AG and Steinmann L, Arylamine acetylation in human red blood cells. *Am Soc Clin Invest* **41**: 1387, 1962.
36. Mondelbaum-Shavit F and Blondheim SH, Acetylation of *p*-aminobenzoic acid by human blood. *Biochem Pharmacol* **30**: 65–69, 1981.
37. Lambie DG and Johnson RH, Drugs and folate metabolism. *Drugs* **30**: 145–155, 1985.
38. In: *Nutritional Biochemistry*, pp. 355–376. pub. Academic Press Inc.
39. da Costa M and Iqbal MP, The transport and accumulation of methotrexate in human erythrocytes. *Cancer* **48**: 2427–2432, 1981.
40. Benesch RE, Kwang S, Benesch R and Baugh CM, The binding of folyl and antifolylpolyglutamates to haemoglobin. *J Biol Chem* **260**: 14653–14658, 1985.
41. Hilton JG, Cooper BA and Rosenbault DS, Folate polyglutamate synthesis and turnover in cultured human fibroblasts. *J Biol Chem* **254**: 8398–8403, 1979.
42. Shin YS, Buehring KU and Stokstad ELR, Studies of folate compounds in nature. *Arch Biochem Biophys* **163**: 211–224, 1974.
43. Murphy M, Keating M, Boyle P, Weir DG and Scott JM, The elucidation of the mechanism of folate catabolism in the rat. *Biochem Biophys Res Commun* **71**: 1017–1024, 1976.
44. McPartlin J, Courtney G, McNulty H, Weir D and Scott J, The quantitive analysis of endogenous folate catabolites in human urine. *Anal Biochem* **206**: 256–261, 1992.
45. Murphy M and Scott JM, The turnover catabolism and excretion of folate administered at physiological concentrations in the rat. *Biochem Biophys Acta* **583**: 535–539, 1979.
46. Saleh AM, Pheasant AE, Blair JA and Allan RN, The effects of malignant disease on the metabolism of pteroylglutamic acis in man. *Biochem Soc Trans* **8**: 566–567, 1980.
47. McPartlin J, Halligan A, Scott JM, Darling M and Weir DG, Accelerated folate breakdown in pregnancy. *Lancet* **341**: 148–149, 1993.
48. Minchin RF, Acetylation of para-aminobenzoylglutamate, a folate catabolite, by recombinant human *N*-acetyltransferase and U937 cells. *Biochem J* **307**: 1–3, 1995.
49. Zaher H and Svensson CK, Glucocorticoid induction of hepatic acetyl-CoA: Arylamine *N*-acetyltransferase activity in the rat. *Res Commun Chem Pathol Pharmacol* **83**: 195–208, 1994.
50. Derewlany LO, Knie B and Koren G, Arylamine *N*-acetyltransferase activity of the human placenta. *J Pharmacol Exp Ther* **269**: 756–765, 1994.
51. Derewlany LO, Knie B and Koren G, Human placental transfer and metabolism of *p*-aminobenzoic acid. *J Pharmacol Exp Ther* **269**: 761–765, 1994.